Title
LOW TEMPERATURE DISLOCATION MECHANISMS IN ORDERED AND DISORDERED CugAu

Authors
Langdon, Terence G.
Dorn, John E.

Publication Date
1967-10-01

UCRL-17863

c. 2

University of California

Ernest O. Lawrence Radiation Laboratory

LOW TEMPERATURE DISLOCATION MECHANISMS IN ORDERED AND DISORDERED Cu_3Au

Terence G. Langdon and John E. Dorn

October 1967

DISCLAIMER

Submitted to Phil. Mag.

UCRL-17863
Preprint

UNIVERSITY OF CALIFORNIA

Lawrence Radiation Laboratory
Berkeley, California

AEC Contract No. W-7405-eng-48

LOW TEMPERATURE DISLOCATION MECHANISMS IN ORDERED AND DISORDERED Cu_3Au

Terence G. Langdon† and John E. Dorn††

October, 1967

†Research Fellow of the Inorganic Materials Research Division of the Lawrence Radiation Laboratory, University of California, Berkeley.

††Professor of Materials Science, Department of Mineral Technology, College of Engineering, and Research Metallurgist of the Inorganic Materials Research Division of the Lawrence Radiation Laboratory, University of California, Berkeley.

UCRL-17863

LOW TEMPERATURE DISLOCATION MECHANISMS IN ORDERED AND DISORDERED Cu_3Au

Terence G. Langdon and John E. Dorn

Inorganic Materials Research Division, Lawrence Radiation Laboratory, and Department of Mineral Technology, College of Engineering, University of California, Berkeley, California

October, 1967

ABSTRACT

The temperature and strain rate dependence of the flow stress of ordered and disordered polycrystalline Cu_3Au was investigated in the range 20° - 420°K. A thermally activated deformation mechanism was observed at temperatures less than ∿ 100°K and ∿ 340°K for the ordered and disordered material respectively. For ordered Cu_3Au, the experimental data were shown to correlate well with the requirements of the Peierls mechanism over the entire thermally activated region; for the disordered material, good agreement was only obtained at temperatures less than ∿ 120°K, and it appeared that deformation was by the intersection mechanism in the temperature range ∿ 220° - 340°K.

It is suggested that a pseudo-Peierls mechanism occurs in ordered Cu_3Au at temperatures less than ∿ 100°K, and in disordered Cu_3Au at temperatures less than ∿ 120°K, due to splitting of the cores of screw dislocations on several planes.

I. INTRODUCTION

In an investigation of the influence of long-range order upon strain-hardening, Davies and Stoloff (1965) showed that the critical resolved shear stress for yielding of ordered Cu_3Au remained approximately constant as the temperature was decreased toward 77°K, whereas that for disordered Cu_3Au exhibited a rather pronounced increase for a face centered cubic material. This suggests that the low temperature deformation mechanisms for the disordered Cu_3Au might be significantly different from that for face centered cubic alloys in general, and also from that operative in the ordered state. Consequently, the present investigation was undertaken with the specific objective of obtaining detailed information on the activation energies and volumes for the low temperature deformation mechanisms of both disordered and ordered Cu_3Au. The results to be presented strongly support the thesis that the low temperature behavior of these alloys follow the Peierls mechanism, and that, in addition, the disordered alloy obeys the intersection mechanism at intermediate temperatures. At higher temperatures, both states exhibit the usual athermal mechanical behavior.

II. EXPERIMENTAL TECHNIQUES

The alloys were prepared in the form of 0.125 in. diameter drawn rods containing 50.85 ± 0.05 weight percent Au. Spectrochemical analyses gave 0.04 weight percent Ag as the only detectable impurity; the balance was Cu. Two inch long test specimens were machined from the rods to give a 0.68 in. gage section having a diameter of 0.085 in.

The disordered state was achieved by annealing under argon at 1000°K

for 30 minutes, slow furnace cooling to 725°K and then water quenching. Specimens for the ordered state were also annealed under argon at 1000°K for 30 minutes, furnace cooled below the ordering temperature (663°K) to 643°K, held at this temperature for 85 hours, and then slowly cooled ($\sim$ 3°K per hour) to 473°K and rapidly cooled ($\sim$ 100°K per hour) to room temperature. Roessler et al. (1963) have shown that such treatment produces a high degree of long-range order, with a long-range order parameter of S $\sim$ 0.87. Metallographic examination following etching with a 50% aqueous solution of I_2 in KI revealed that both the disordered and ordered states had the same equiaxed grain size of $\sim$ 630 grains per centimeter.

All specimens were tested in tension using an Instron machine. For tests above room temperature the specimens were totally immersed in a silicone oil bath controlled to an accuracy of $\pm$ 0.5°K. Over the range from 273° to 77°K the specimens were tested while fully immersed in constant temperature baths. Tests below 77°K were carried out in a specially designed helium cryostat.

To insure uniformity from specimen to specimen, and to place them in substantially the same state, each specimen was first prestrained to a fixed flow stress at 300°K at a shear strain rate of $\dot{\gamma} = 3.64 \times 10^{-5}$ per sec. The standard states were selected to be a flow stress of 7.23×10^8 and 5.10×10^8 dynes per square centimeter for the disordered and ordered states respectively. Immediately following the prestrain, each specimen was brought to the desired temperature and pulled in tension at either $\dot{\gamma}_1 = 3.64 \times 10^{-6}$ per sec or $\dot{\gamma}_2 = 3.64 \times 10^{-4}$ per sec. Stresses

and temperatures are estimated to be within ± 0.1 x 10^8 dynes per square centimeter and ± 1°K respectively of the reported values. The shear strain rate was taken as $\dot{\gamma} = 3/4\ \dot{\varepsilon}$ and the applied shear stress as $\tau = \sigma/2$, where $\dot{\varepsilon}$ and σ are the tensile strain rate and tensile stress respectively. The shear stress corresponding to the point at which flow was initiated was determined by taking a $\gamma = 1 \times 10^{-4}$ offset from the modulus line.

III. EXPERIMENTAL RESULTS

The stress-strain curves for the disordered and ordered material, of which typical examples at different temperatures are shown in Fig. 1, revealed a sharp increase in the flow stress for the disordered material at temperatures less than about 340°K and for the ordered material at temperatures less than about 100°K. This is clearly revealed by plotting the experimentally determined flow stresses, τ, as functions of temperature and strain rate, as shown in Fig. 2. In the present investigation, both the ordered and disordered states exhibit a thermally activated dislocation mechanism over the lower temperature range, as revealed by the fact that their flow stresses decrease with increasing temperatures and decreasing strain rates. Over the higher temperature range, however, their behavior is athermal, as documented by the gradual linear decrease in flow stress with increasing temperature and the insensitivity of the flow stress to strain rate. Above about 360°K, the disordered alloy exhibited a serrated stress-strain curve (Fig. 1) indicating the introduction of the Portevin-Le Chatelier effect. For the same test conditions, the flow stress for the disordered state always exceeded that for the

ordered state.

Over the athermal range, the flow stress, τ_A, varies with temperature, T, in a manner that parallels the variation of the shear modulus, G, according to

$$\tau_{A(T)} = \tau_{A(365^\circ K)} \frac{G_T}{G_{365^\circ K}} \qquad (1)$$

where 365°K is a temperature chosen to be within the athermal region. Applying the single crystal data obtained by Flinn et al. (1966), for G on the (111) plane in the [110] direction as a function of temperature, gave the straight lines shown through the higher temperature flow stress data of Fig. 2. It is obvious that Eq. (1) is well-satisfied over the athermal region. The somewhat low value of the yield stress at about 410°K for the disordered state is probably due to recovery.

The effective stress required to assist thermal activation of the rate controlling mechanism, τ^*, defined by

$$\tau^* = \tau - \tau_A \qquad (2)$$

is given in Fig. 3 by subtracting the athermal stress from the total flow stress.

At low temperatures, each thermally activated dislocation mechanism is usually well represented by a relationship of the form

$$\dot{\gamma} = \dot{\gamma}_o \exp\left(-U\{\tau^*\}/kT\right) \qquad (3)$$

where $\dot{\gamma}_o$ is a frequency factor, U is the activation energy and kT has the usual meaning of the Boltzmann constant times the absolute temperature. In general the activation energy depends on the effective stress, τ^*, and on the shear modulus of elasticity, G, according to

$$U\{\tau^*\} = (G/G_o)\, U_o\{\tau^*\} \tag{4}$$

where the subscript zero refers to the absolute zero of temperature. Whereas the activation energy is independent of substructural details for some mechanisms (e.g. the Peierls), it depends on such factors in other mechanisms (e.g. the intersection mechanism). The frequency factor, $\dot{\gamma}_o$, is linearly related to the density of the mobile dislocations and is always insensitive to T and usually independent of the effective stress, τ^*.

One feature of significance in identifying mechanisms is the functional dependence of the activation energy on τ^*. The apparent activation energy is defined by

$$q = \frac{\partial \ell n \dot{\gamma}}{\partial -(1/kT)} = (G/G_o)\, U_o\{\tau^*\} - T \frac{\partial (G/G_o)}{\partial T} U_o\{\tau^*\} \simeq U_o\{\tau^*\} \tag{5}$$

where the second equality follows upon introduction of Eqs. (3) and (4), and the third results from the well-known approximation that $G - T\partial G/\partial T \simeq G_o$. The apparent activation energies deduced from the data of Fig. 3 are shown as functions of τ^* in Fig. 4.

A partial check on the internal consistency of the above assumptions can be made by ascertaining whether $U\{\tau^*\}$ increases linearly with T

at a constant strain rate $\dot{\gamma}$ as required by Eq. (3). For this purpose, $U\{\tau^*\}$ was determined from the values of $U_o\{\tau^*\}$ given in Fig. 4 by application of Eq. (4), and plotted as a function of T as shown in Fig. 5. Whereas the ordered Cu_3Au exhibits the theoretically justified linear increase of $U\{\tau^*\}$ as a function of T, the disordered alloy exhibits two linear regions (I and II) with a transition between them. Since the slope of the $U\{\tau^*\}$ - T lines is $k \ln \dot{\gamma}_o/\dot{\gamma}$, it follows that $\dot{\gamma}_o$ is appreciably smaller for Region II than for Region I. This suggests that a transition occurs in the disordered alloy between 120°K and 225°K from a lower temperature mechanism to a higher temperature mechanism having a smaller value of $\dot{\gamma}_o$. Additional evidence for this transition will be presented later.

Although the shapes of the τ^* - T curves of Fig. 3 and the $U_o\{\tau^*\}$ - τ^* curves of Fig. 4 are dependent on the operative mechanisms, they seldom permit a unique identification of the mechanism per se. A more detailed insight is obtained from the apparent activation volume, v, defined by

$$v = kT \frac{\partial \ln \dot{\gamma}}{\partial \tau^*} = kT \frac{\partial \ln \dot{\gamma}_o}{\partial \tau^*} - \frac{\partial U\{\tau^*\}}{\partial \tau^*} \qquad (6a)$$

or the true activation volume, v^*, defined by

$$v^* = - \frac{\partial U\{\tau^*\}}{\partial \tau^*} \qquad (6b)$$

When, as is generally true for low temperature dislocation mechanisms, $\dot{\gamma}_o$ is insensitive to τ^*, the true activation volume can be deduced from either

$$v_A^* = kT \frac{\partial \ell n \dot{\gamma}}{\partial \tau^*} \text{ or } v_B^* = - \frac{\partial U\{\tau^*\}}{\partial \tau^*} \qquad (6c)$$

Activation volumes obtained in these ways are presented as functions of τ^* in Fig. 6, with one ordinate marked in terms of b^3, where b, the Burgers vector, is taken as $a/2[\bar{1}10]$. The agreement between v_A^* and v_B^* is good for the ordered alloy over the entire range. For the disordered alloy the agreement is good at the higher values of τ^*, but there appears to be some deviation at the lower values corresponding to the transition region of Fig. 5.

The low activation volumes obtained for the ordered Cu_3Au, and for the disordered alloy over Region I, are suggestive of either a Peierls mechanism (Peierls 1940) or the Fleischer mechanism of interactions between dislocations and impurity atoms (Fleischer 1962). Fleischer suggested that the rapid increase in the yield strength of b.c.c. metals with decreasing temperatures, and the small activation volumes they exhibit, might be ascribed to appropriately dilute concentrations of impurity atoms; with some exceptions (Koo 1963, Stein and Low 1966, Stein 1967), however, the weight of current evidence suggests that the τ^* - T and v^* - τ^* relationships are independent of impurity concentrations. Although these observations appear to disqualify the operation of the Fleischer theory, they are wholly in agreement with the requirements of the Peierls theory. It is highly unlikely that the low temperature behavior of the ordered and disordered Cu_3Au alloy under study here might be ascribed to impurity effects. Furthermore, such impurities, if present, should have approximately the same concentrations in the ordered and

disordered state. Obviously the observed differences between the low temperature $\tau^* - T$ curves for the ordered and disordered alloys cannot be rationalized in terms of interactions between impurity atoms and dislocations. However, as will be demonstrated later, the low temperature behavior of ordered Cu_3Au, and the disordered Cu_3Au in Region I, is in good agreement with the Peierls mechanism.

The difference in behavior of disordered Cu_3Au (vide Fig. 5) in Region II as contrasted to Region I is further reflected in major differences in the activation volume. As shown in Fig. 6, the activation volumes for the disordered alloy over the lower values of τ^* (or higher values of T) are much greater than permissible for the Peierls mechanism. In fact, they begin to approach those that might be expected for the dislocation intersection mechanism.

Additional insight into low temperature mechanisms is obtained by studying the effect of straining on v_A^*. Typical examples of the variation of v_A^* with strain, as deduced from $kT\,\Delta \ell n \dot{\gamma}/\Delta\tau$ by changing the strain rate periodically during deformation, are shown in Fig. 7. The solid symbol, at $\gamma = 0$, represents the value from the yield stress data as given in Fig. 6. In all examples this agreed well with the values of v_A^* obtained at low strains by periodic changes in $\dot{\gamma}$. The value of v_A^* for ordered Cu_3Au and that for the disordered alloy over Region I was, excepting for some scatter, independent of the strain. This is consistent with the concept that the Peierls mechanism controls the deformation over the pertinent ranges. In contrast, the activation volume for the disordered alloy in Region II, and for the transition region also,

decreased significantly with straining. This obviously infers that the effective barriers in Region II for the disordered alloys are localized and that their number increases with strain. The most likely process in this region is the thermally activated cutting of forest dislocations.

IV. ANALYSIS

The experimental results strongly suggest that the Peierls mechanism is operative in ordered and disordered Cu_3Au at temperatures less than $\sim 100^\circ K$ and $\sim 120^\circ K$ respectively. Although a number of models have been suggested for the Peierls process, the analysis presented here will be confined exclusively to the Dorn and Rajnak model (1964); this model has been shown to agree well with the experimental results obtained for a number of b.c.c. and h.c.p. materials (Guyot and Dorn 1967).

In the theory, as modified slightly by Guyot and Dorn (1967), the shear strain rate is given by

$$\dot{\gamma} = \frac{\rho L a b^2 \nu}{2w^2} \exp\left(-U_n\{\tau^*\}/kT\right) \qquad (7)$$

where ρ = density of mobile dislocations,

L = mean length swept out by a pair of kinks before they become arrested at an obstacle,

a = distance between Peierls valleys,

b = Burgers vector,

ν = Debye frequency,

U_n = critical energy for nucleation of a pair of kinks,

w = width of a pair of kinks at the critical energy U_n.

Over the thermally activated region, τ^* decreases with increasing temperature and becomes zero at a critical temperature T_c. At this temperature, $U_n = 2U_k$ where U_k is the energy of a single kink, and Eq. (7) becomes

$$\dot{\gamma} = \frac{\rho L a b^2 \nu}{2w^2} \exp\left(-2U_k/kT_c\right) \tag{8}$$

At absolute zero, the Peierls stress τ_p^o is the stress needed to initiate deformation. At higher temperatures, the Peierls stress is assumed to vary with temperature as does the shear modulus, and thus

$$\tau_p = (G/G_o)\, \tau_p^o \tag{9}$$

According to the theory of Dorn and Rajnak (1964), there is a relationship between τ^* and U_k such that, at constant $\dot{\gamma}$,

$$\frac{\tau^*}{\tau_p} = \frac{\tau^*}{\tau_p^o}\,(G_o/G_T) = f\left(\frac{Un}{2U_k}\right) = f\left(\frac{T}{T_c}\right) \tag{10}$$

It is not easy to obtain precise values for τ_p^o directly from Fig. 1, its evaluation requires an extrapolation from about 20°K to 0°K. Although the values of the critical temperatures can be obtained directly for the ordered alloy, they cannot be measured directly for the disordered alloy because of the intrusion of the intersection mechanism over Region II. A method used by Lau et al. (1967) was therefore employed, in which the theoretical curves for sinusoidal Peierls hills of τ^*/τ_p vs. $U_n/2U_k$ ($\simeq T/T_c$) were plotted on logarithmic scales. For each strain rate, the values of $\tau^*(G_o/G_T)$ were then plotted on the same scale, and superimposed

to give the best coincidence for the ordered and disordered material respectively. The deduced values for τ_p° and T_c are shown in Table I. For the ordered material, good agreement was obtained over the whole thermally-activated region; for the disordered material, however, there was a deviation from the Peierls mechanism at the higher temperatures, as shown in Fig. 2 where the low temperature region has been extrapolated to the values for T_{c1} and T_{c2} for the assumed Peierls mechanism.

U_k was also determined from the values of the critical temperatures at the two different strain rates, since, as shown by Eq. (8),

$$\frac{\dot{\gamma}_1}{\dot{\gamma}_2} = \frac{\exp\ (-2U_k/kT_{c1})(G_1/G_o)}{\exp\ (-2U_k/kT_{c2})(G_2/G_o)} \tag{11}$$

where G_1 and G_2 are the shear moduli at T_{c1} and T_{c2} respectively. These values are shown in column 4 of Table 1.

Using the values deduced for the critical temperatures, the plots of $\tau^*/\tau_p^\circ \times G(0)/G(T)$ vs. T/T_c, as calculated from the original data, are shown in Fig. 8, together with the theoretical curve for the Peierls mechanism. The agreement with the predictions arising from the Peierls mechanism is good over a wide temperature range, but clearly deviates in the disordered material at the higher temperatures where the intersection mechanism is obtained. A somewhat similar deviation from the dictates of the simple Peierls theory over a higher temperature range has been reported in Fe (Keh and Nakada 1967), in some Fe alloys (Wynblatt et al. 1965, Wynblatt and Dorn 1966, Rawlings and Newey 1967), and, to a minor degree, in Mo (Lau et al. 1967). In the case of the Fe alloy

(Wynblatt and Dorn 1966), however, the higher temperature mechanism was shown not to arise from the intersection of glide with forest dislocations.

Since several other mechanisms also reveal somewhat similar $\tau^* - T$ curves, the Peierls mechanism cannot be confirmed from Fig. 8 alone. The most distinctive characteristic of the Peierls mechanism is a small activation volume which increases somewhat with decreasing τ^* (Fig. 6) and is independent of strain (Fig. 7). The theoretical expression for the activation volume in the Peierls mechanism is given by

$$v_p^* = - \left(\frac{\partial U_n}{\partial \tau^*}\right)_T = - \frac{2U_k}{\tau_p} \frac{\partial (U_n/2U_k)}{\partial (\tau^*/\tau_p)} \qquad (12)$$

A direct comparison of the experimental results with the Dorn and Rajnak model is possible by plotting $(\tau_p/2U_k)v_p^*$ against τ^*/τ_p^o (corrected for the change in shear modulus with temperature). Using the values of τ_p^o and U_k shown in Table 1, and the values of v_A^* from Fig. 6, the result is shown in Fig. 9, together with the theoretical curves for sinusoidal Peierls hills ($\alpha = 0$) and perturbations therefrom ($\alpha = +1, -1$). The agreement with theory is good, except for the disordered material at low values of τ^* (i.e. in Region II).

A further check on the correlation with the theoretical model is possible, by comparing the line energy Γ_o of a dislocation which, according to the theory, is related to U_k and τ_p by

$$\frac{2\pi U_k}{a\Gamma_o} = 5.67 \sqrt{\frac{\tau_p^* ab}{\pi \Gamma_o}} \qquad (13)$$

with the Nabarro estimate of $\Gamma_o = G_o b^2/2$, as shown in columns 5 and 6 respectively of Table 1. The values of $2\Gamma_o/G_o b^2$ are slightly greater than unity, and a similar trend has been observed for other materials (Guyot and Dorn 1967); this suggests that $G_o b^2/2$ underestimates the line energy, probably because it makes no allowance for anisotropy and does not include the energy of the dislocation core. Reasonable agreement between Γ_o and $G_o b^2/2$ is only realized if the Burgers vector is taken as that of the undissociated dislocation. Taking the Burgers vector for a partial dislocation ($b = a/\sqrt{6}$) yields very high values for $2\Gamma_o/G_o b^2$ ($\sim$ 124 for the disordered material), which suggests that the two partials of the dissociated dislocation move together as a unit.

The values of $\rho L/w^2$ in Table 1 were calculated from Eq. (8), using the Debye temperature of Flinn et al. (1960). According to Guyot and Dorn (1967), w may be considered a constant approximated by

$$w = \frac{\pi}{2}\left(\frac{2a\Gamma_o}{b\tau_p}\right)^{1/2} \qquad (14)$$

The values of ρL calculated from this relationship have a reasonable magnitude, as shown in Table 1, and are intermediate between those previously reported for a Mg - 14% Li - 1.5% Al alloy (0.9 cm^{-1})(Abo-el-Fotoh et al. 1967) and AgMg (227 cm^{-1})(Mukherjee and Dorn, 1964).

In every respect the thermally activated mechanisms of slip in ordered Cu_3Au and in the disordered alloy over Region I therefore agree well with the requirements of the Peierls mechanism.

The behavior of the disordered Cu_3Au over Region II appears to be

controlled by the intersection mechanism; the evidence favoring this conclusion centers primarily about the reasonable magnitude of the activation volume and its appropriate decrease with strain. The range of conditions, both T and τ^*, over which this mechanism is controlling, however, was too limited to permit a sufficiently detailed investigation to provide a complete picture of the mechanism. Assuming that the mechanism is that for intersection of dislocations, it is anticipated that the force-displacement diagram will involve that for constriction of the partial dislocations plus that for forming a jog. Consequently, the activation energy will not decrease linearly with τ^*. As a crude estimate, therefore, we might suggest that the activation volume for the lower values of τ^* approaches $v^* = Lbd$, where L is the mean distance between the forest dislocations and d is only slightly less than the equilibrium separation of the partial dislocations ($\sim$ 17 - 36Å)(Marcinkowski 1963). Introducing $d \simeq 10\ b$, we obtain the not unreasonable density of forest dislocations of $\rho = 1/L^2 = b^2d^2/v^{*2} \simeq 5 \times 10^{10}\ cm^{-2}$.

V. DISCUSSION

The conclusion that the deformation of ordered Cu_3Au up to about 100°K and the disordered alloy (over Region I) up to about 120°K is controlled by the thermally activated Peierls mechanism is inevitable in terms of the substantial evidence for this interpretation that was marshalled in the preceeding sections of this report. This conclusion, especially in the case of the disordered alloy, contrasts with the widely documented evidence that the Peierls stress for f.c.c. metals is so low that their deformation at low temperatures is controlled by the thermally activated

dislocation intersection mechanism. The present authors have uncovered only one possible exception to this generalization, which is suggested by the recent report of Zerwekh and Scott (1967) on the low temperature deformation mechanisms in polycrystalline thorium. In that work, however, Zerwekh and Scott interpreted their observation of a rather rapid increase in τ^* with decreasing temperature, low activation volumes ($\sim 40\ b^3$) and the invariance of the activation volumes with strain, as a result of thermal activation of dislocations past strain centers due to interstitial impurities that were known to be present in their material. On the other hand, their data might have been equally interpreted in terms of a Peierls mechanism. Consequently, the operative low temperature deformation mechanism in thorium appears to closely parallel that observed for b.c.c. metals. Recent evidence on b.c.c. materials (Bowen et al. 1967, Keh and Nakada 1967), however, even more strongly supports the thesis first presented by Conrad (1963) that interstitial impurities serve principally to increase the athermal stress level, and that the effective stress for the thermally activated mechanism is independent of impurity content and is determined primarily by a Peierls mechanism. The issue relative to thorium will only be resolved following tests to ascertain whether the $\tau^* - T$ curve is reduced, and the $v^* - \tau^*$ curve is appropriately increased, as a result of purification. For the Cu_3Au alloys, however, it is much more certain that the low temperature thermally activated deformation mechanisms are controlled by the Peierls mechanism.

At first sight it is strange that the Peierls stress is significantly

higher for the disordered alloy than for the ordered alloy. If, for example, the impurity solute atom mechanism controlled, it would be expected that τ^* at 0°K would be about the same for both the ordered and disordered states. Furthermore, if a simple true Peierls mechanism were operative, the Peierls stress for the ordered alloy should, because of the higher regularity of the lattice, have exceeded that for the disordered state. On this basis it seems that the simple pure Peierls mechanism, where the dislocation core is uniformly spread out on the operative slip plane, cannot account for all of the results. The differences in the Peierls stress for the ordered and disordered states, however, are qualitatively consistent with expectations arising from the pseudo-Peierls process (Dorn 1967). This process is based on the possibility that the cores of dislocations in screw orientation might dissociate on other than the primary slip plane and thereby further lower the energy of the dislocation. In the ordered alloy the dissociation of the core would be more resistricted than in the disordered alloy since, in addition to the stacking fault energies, the antiphase boundary energy would contribute to reduce the separation of the partial dislocations. This, in effect, would be equivalent to reducing the height of the Peierls hill and therefore the Peierls stress.

The question now arises as to the kind of dissociation that must be considered in order to account for the observed results. It is, of course, not possible to give an unambiguous answer at this time, since much more need be known about dislocation core splitting before this problem can be approached with assurance. It is interesting, however, to

view one of several possibilities, not so much from the viewpoint that it is significant but more that it (and several others) appear to need more detailed study. Marcinkowski, Brown and Fisher (1961) have clearly shown that an $a[\bar{1}10]$ superdislocation on the (111) plane in the ordered Cu_3Au splits on its slip plane into two sets of $a/2[\bar{1}10]$ dislocations separated by an antiphase boundary. Each $a/2[\bar{1}10]$ dislocation, however, further splits into the standard partial dislocations $a/6[\bar{2}11]$ and $a/6[\bar{1}2\bar{1}]$, separated by a stacking fault the energy of which is further augmented by an antiphase boundary energy. The $a/2[\bar{1}10]$ dislocation in the disordered alloy undertakes the same dissociation into partial dislocations separated only by a stacking fault. All of these dissociations take place on the (111) plane and the partial dislocations are so well separated that the cores of adjacent partial dislocations do not overlap. It therefore appears that an acceptable pseudo-Peierls mechanism might involve the dissociation of, for example, the $a/6[\bar{2}11]$ dislocation in screw orientation. Although other dissociations are possible, consider the reaction

$$\underset{(111)}{a/6[\bar{2}11]} \rightarrow \underset{(01\bar{1})}{a/6[\bar{2}00]} + \underset{(102)}{a/6[010]} + \underset{(\bar{1}20)}{a/6[001]} \qquad (15)$$

where the dissociation planes are designated below the Burgers vectors of the dislocations. Using the usual expression of $\Gamma_o \simeq G_o b^2/2$, it appears that the change in energy for the proposed reaction is zero and therefore, on this basis, cannot take place. This, however, need not be so under special circumstances if the anisotropic line energies were

evaluated. Furthermore, as mentioned previously, the pseudo-Peierls mechanism is only concerned with small splittings of the cores of screw dislocations on several planes. Thus, such splittings become possible with a reduction in energy even when the long range line energy change might be zero; consequently, the operation of the pseudo-Peierls mechanism cannot yet be disqualified for the above example of dissociation.

V. CONCLUSIONS

1. Ordered and disordered polycrystalline Cu_3Au exhibit a thermally activated deformation mechanism at temperatures less than $\sim$ 100°K and $\sim$ 340°K respectively.

2. An analysis of the experimental data in terms of the Peierls mechanism suggests good agreement for the ordered material below the athermal region, and for the disordered material at temperatures less than $\sim$ 120°K. Between $\sim$ 225°K and $\sim$ 340°K, it is suggested that the disordered material deforms by the intersection mechanism.

3. The Peierls stress, τ_p^o, was estimated to be 6.4×10^8 and 4.2×10^8 dynes per square centimeter for the disordered and ordered material respectively.

4. It is suggested that a pseudo-Peierls mechanism occurs in Cu_3Au due to the splitting of the cores of screw dislocations on several planes.

Table 1. Summary of results

	$\dot{\gamma}$ sec^{-1}	τ_p^o x 10^8 dynes/cm^2	T_c °K	U_k ergs	Γ_o ergs/cm	$2\Gamma_o / G_o b^2$ ergs	$\rho L/w^2$ cm^{-3}	ρL cm^{-1}
Disordered	3.64×10^{-6} 3.64×10^{-4}	6.42	177 240	2.15×10^{-13}	5.46×10^{-4}	4.5	2.87×10^{12}	1.15 x 10
Ordered	3.64×10^{-6} 3.64×10^{-4}	4.19	86 108	1.32×10^{-13}	3.80×10^{-4}	3.0	1.38×10^{13}	6.15 x 10

UCRL-17863

ACKNOWLEDGEMENTS

The authors are grateful to Mr. Osama Abo-el-Fotoh for experimental assistance. This work was supported through the Inorganic Materials Research Division of the Lawrence Radiation Laboratory by the United States Atomic Energy Commission.

REFERENCES

Abo-el-Fotoh, M. O., Mitchell, J. B., and Dorn, J. E., 1967, Lawrence Radiation Laboratory Report No. UCRL-17769, University of California, Berkeley.

Bowen, D. K., Christian, J. W., and Taylor, G., 1967, Canad. J. of Physics, 45, 903.

Conrad, H., 1963, Symposium on the Relation between the Structure and Mechanical Properties of Metals (H.M.S.O.: London), p.476.

Davies, R. G., and Stoloff, N. S., 1965, Phil. Mag., 12, 297.

Dorn, J. E., 1967, Lawrence Radiation Laboratory Report No. UCRL-17521, University of California, Berkeley.

Dorn, J. E., and Rajnak, S., 1964, Trans. Amer. Inst. Min. (Metall.) Engrs., 230, 1052.

Fleischer, R. L., 1962, J. Appl. Phys., 33, 3504.

Flinn, P. A., McManus, G. M., and Rayne, J. A., 1960, J. Phys. Chem. Solids, 15, 189.

Guyot, P., and Dorn, J. E., 1967, Canad. J. of Physics, 45, 983.

Keh, A. S., and Nakada, Y., 1967, Canad. J. of Physics, 45, 1101.

Koo, R. C., 1963, Acta Met., 11, 1083.

Lau, S. S., Ranji, S., Mukherjee, A. K., Thomas, G., and Dorn, J. E., 1967, Acta Met., 15, 237.

Marcinkowski, M. J., 1963, Electron Microscopy and Strength of Crystals (Interscience: New York), p.333.

Marcinkowski, M. J., Brown, N., and Fisher, R. M., 1961, Acta Met., 9, 129.

Mukherjee, A. K., and Dorn, J. E., 1964, Trans. Amer. Inst. Min. (Metall.)

Engrs., 230, 1065.

Peierls, R., 1940, Proc. Phys. Soc., 52, 34.

Rawlings, R. D., and Newey, C. W. A., 1967, Acta Met., 15, 440.

Roessler, B., Novick, D. T., and Bever, M. B., 1963, Trans. Amer. Inst. Min. (Metall.) Engrs., 227, 985.

Stein, D. F., 1967, Canad. J. of Physics, 45, 1063.

Stein, D. F., and Low, J. R., 1966, Acta Met., 14, 1183.

Wynblatt, P., and Dorn, J. E., 1966, Trans. Amer. Inst. Min. (Metall.) Engrs., 236, 1451.

Wynblatt, P., Rosen, A., and Dorn, J. E., 1965, Trans. Amer. Inst. Min. (Metall.) Engrs., 233, 651.

Zerwekh, R. P., and Scott, T. E., 1967, Trans. Amer. Inst. Min. (Metall.) Engrs. 239, 432.

FIGURE CAPTIONS

Figure 1. Typical stress vs. strain curves at different temperatures.

Figure 2. Flow stress vs. temperature, for two different strain rates.

Figure 3. Thermally activated component of the flow stress vs. temperature.

Figure 4. Apparent activation energy vs. thermally activated component of the flow stress.

Figure 5. Activation energy vs. temperature over the thermally activated range.

Figure 6. Activation volumes determined in two ways vs. thermally activated component of the flow stress.

Figure 7. Activation volume vs. true strain at different temperatures.

Figure 8. Thermally activated component of the flow stress vs. temperature in dimensionless units.

Figure 9. Activation volume vs. thermally activated component of the flow stress in dimensionless units.

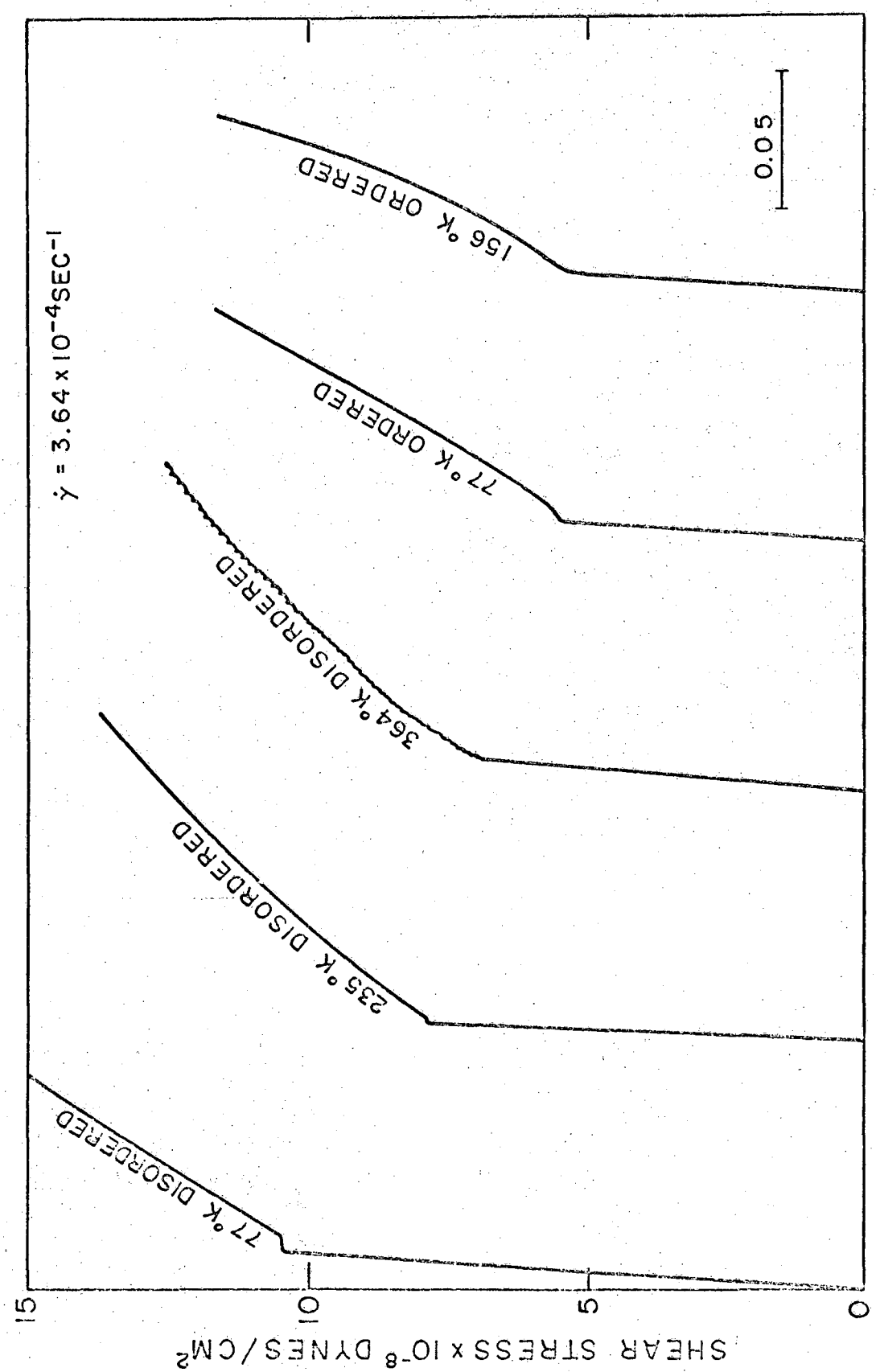
SHEAR STRESS x 10^{-8} DYNES/CM^2
15
10
5
0
STRAIN
$\dot{\gamma} = 3.64 \times 10^{-4} SEC^{-1}$
0.05
156 °K ORDERED
77 °K ORDERED
364 °K DISORDERED
235 °K DISORDERED
77 °K DISORDERED

FIG. 1

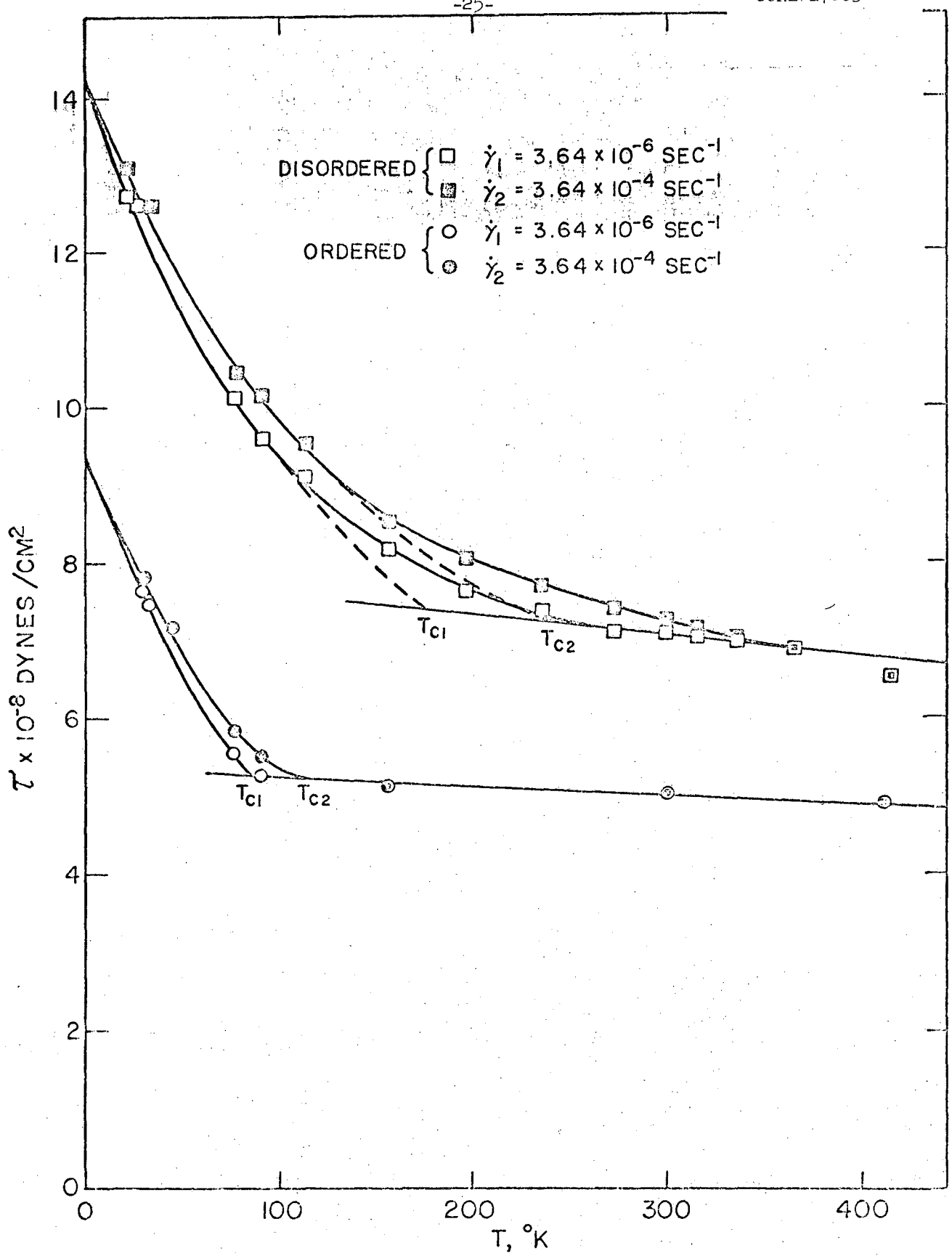
DISORDERED
$\dot{\gamma}_1 = 3.64 \times 10^{-6}$ SEC^{-1}
$\dot{\gamma}_2 = 3.64 \times 10^{-4}$ SEC^{-1}
ORDERED
$\dot{\gamma}_1 = 3.64 \times 10^{-6}$ SEC^{-1}
$\dot{\gamma}_2 = 3.64 \times 10^{-4}$ SEC^{-1}
T_{c1}
T_{c2}
T_{c1}
T_{c2}
$\tau \times 10^{-8}$ DYNES/CM^2
T, °K
0
2
4
6
8
10
12
14
0
100
200
300
400

FIG. 2

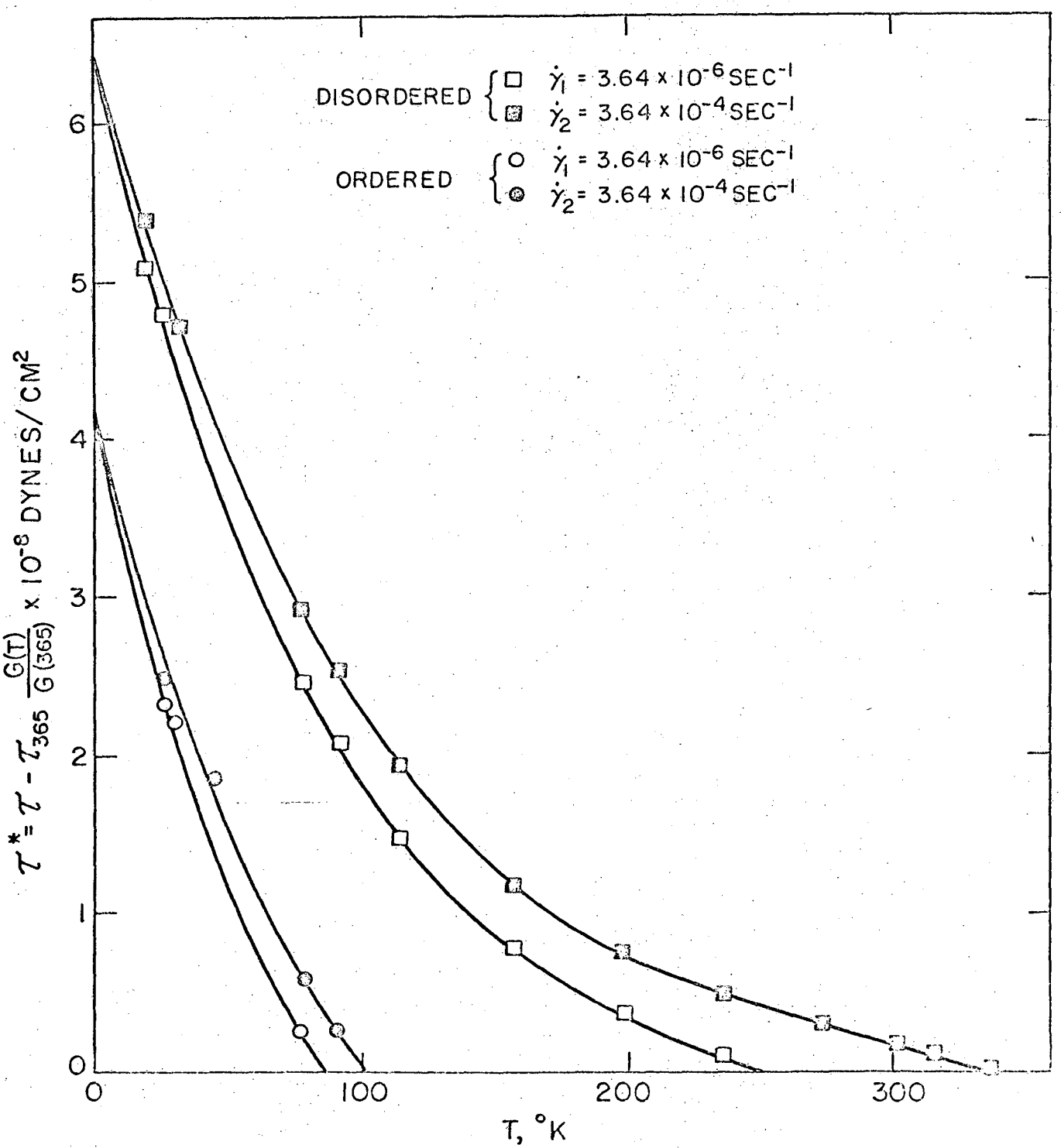
DISORDERED
$\dot{\gamma}_1 = 3.64 \times 10^{-6}\,SEC^{-1}$
$\dot{\gamma}_2 = 3.64 \times 10^{-4}\,SEC^{-1}$
ORDERED
$\dot{\gamma}_1 = 3.64 \times 10^{-6}\,SEC^{-1}$
$\dot{\gamma}_2 = 3.64 \times 10^{-4}\,SEC^{-1}$
$\tau^* = \tau - \tau_{365} \frac{G(T)}{G(365)} \times 10^{-8}$ DYNES/CM^2
T, °K
0
1
2
3
4
5
6
0
100
200
300

FIG. 3

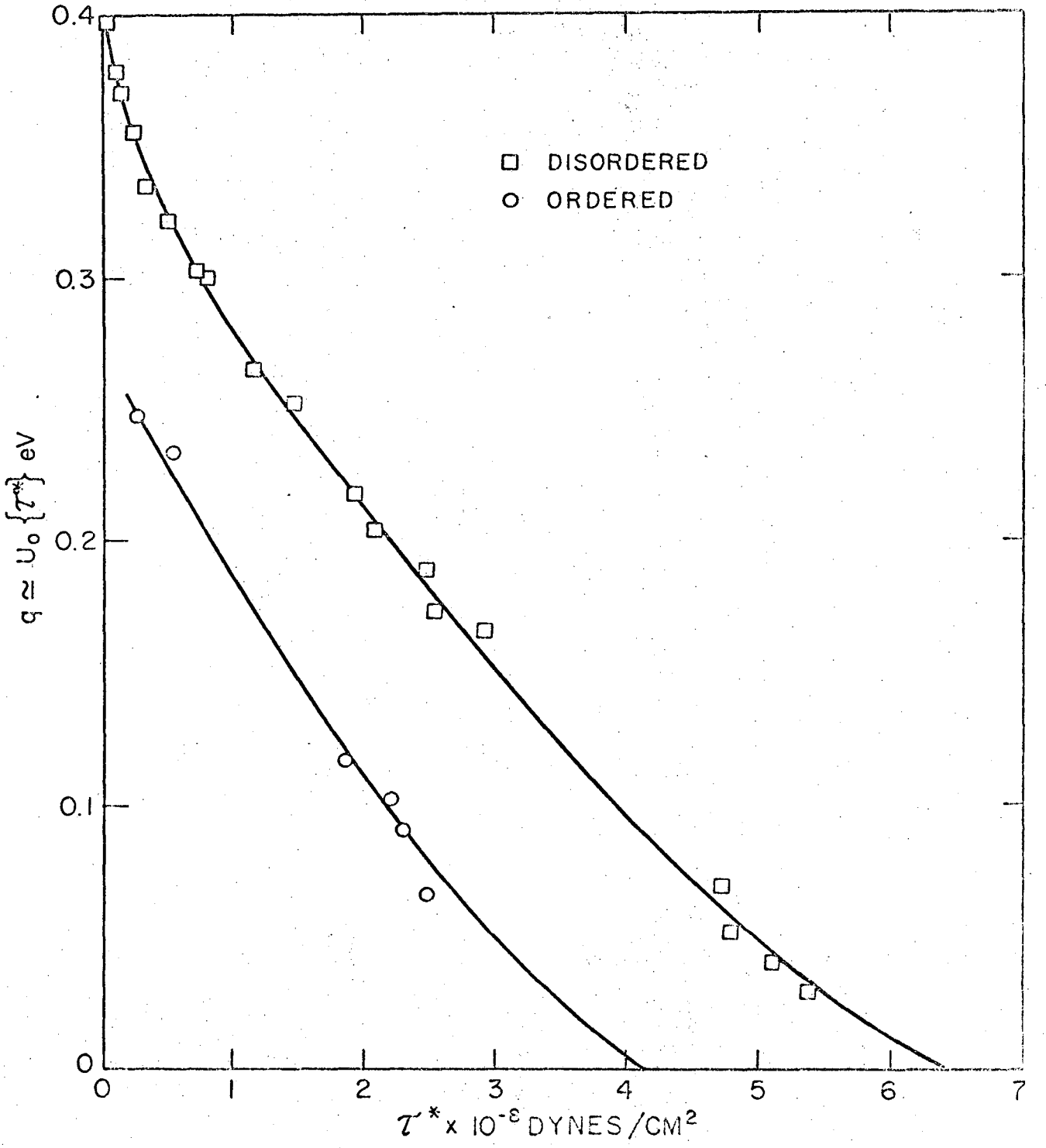
0.4
0.3
0.2
0.1
0
0
1
2
3
4
5
6
7
DISORDERED
ORDERED
q ≃ U₀ {τ*} eV
τ* x 10⁻⁸ DYNES/CM²

FIG. 4

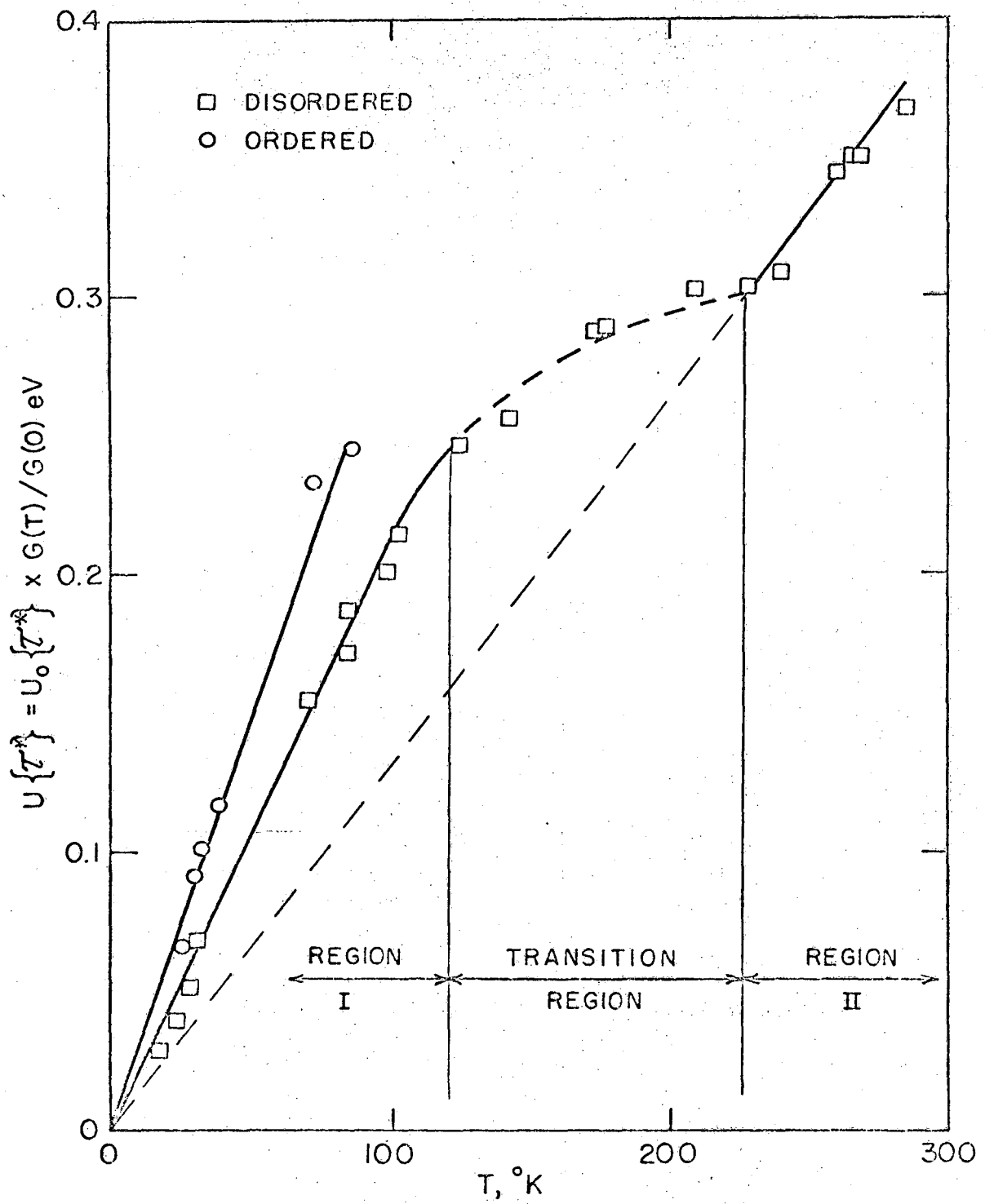
0.4
0.3
0.2
0.1
0
0
100
200
300
T, °K
□ DISORDERED
○ ORDERED
$U\{\tau^*\} = U_0\{\tau^*\} \times G(T)/G(0)$ eV
REGION I
TRANSITION REGION
REGION II

FIG. 5

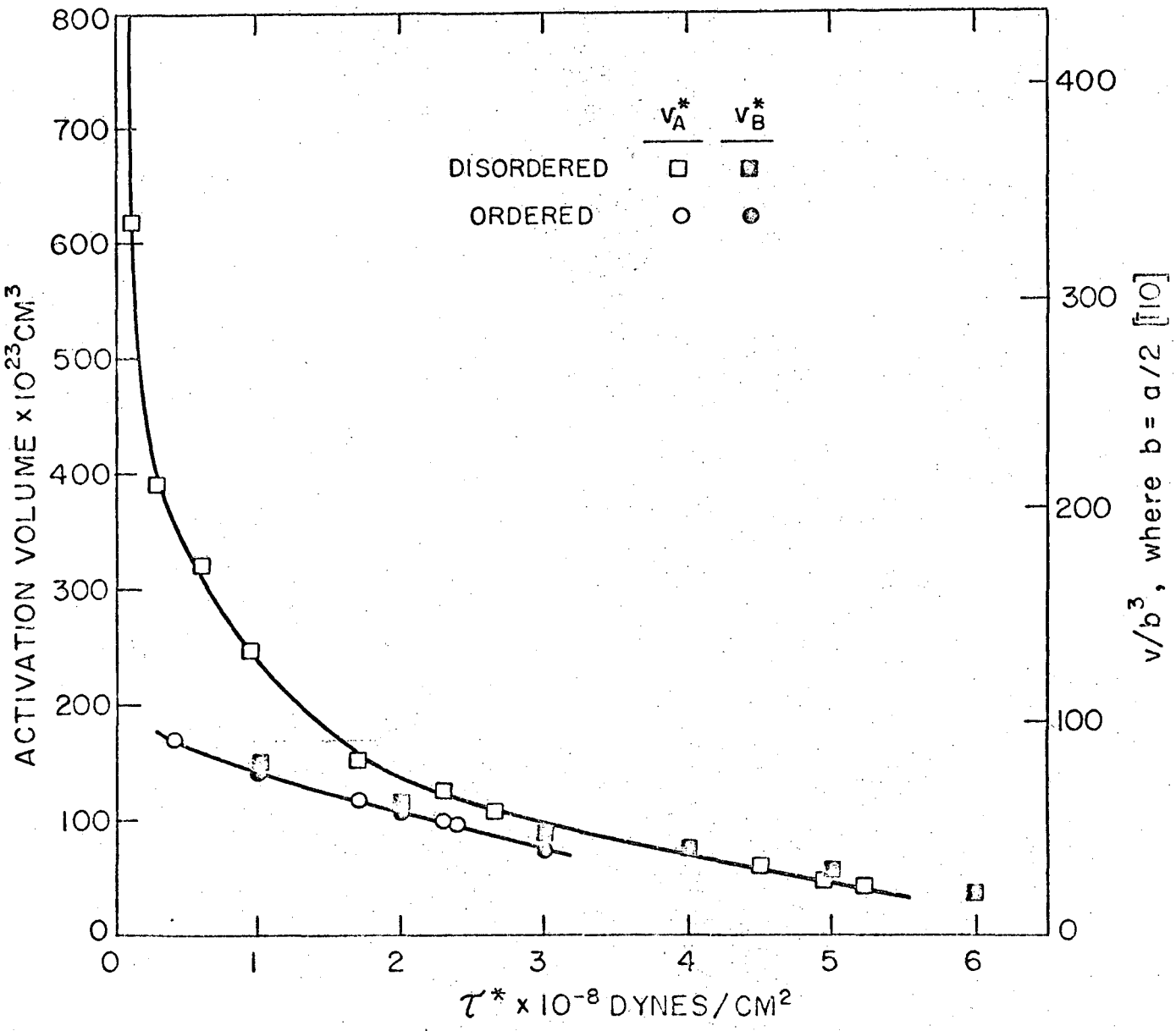
800
700
600
500
400
300
200
100
0
ACTIVATION VOLUME x 10^23 CM^3
400
300
200
100
0
v/b^3, where b = a/2 [110]
0
1
2
3
4
5
6
τ* x 10^-8 DYNES/CM^2
V_A*
V_B*
DISORDERED
ORDERED

FIG. 6

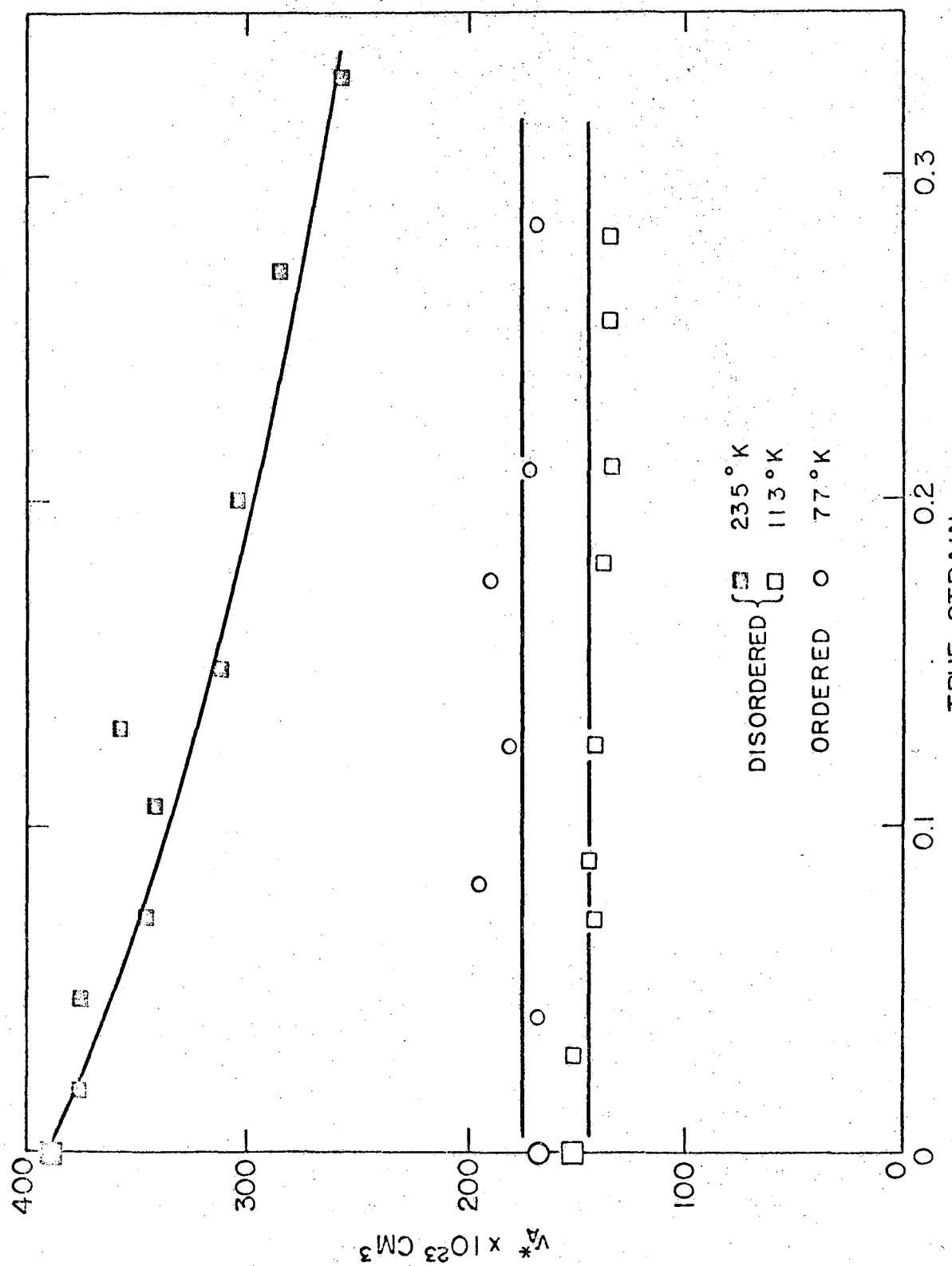
400
300
200
100
0
0
0.1
0.2
0.3
TRUE STRAIN, γ
V_A^* x 10^{23} CM^3
DISORDERED
235 °K
113 °K
ORDERED
77 °K

FIG. 7

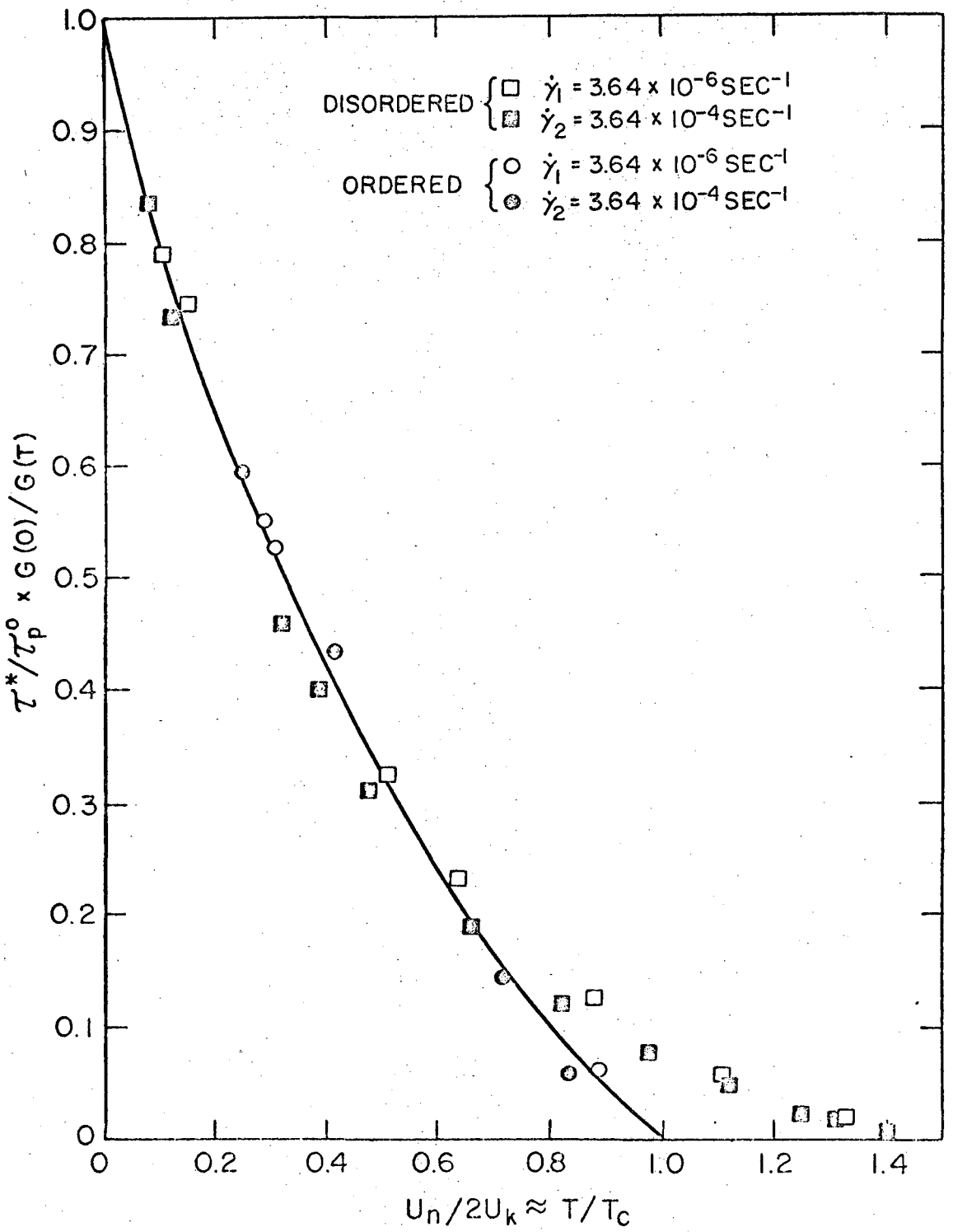
DISORDERED
$\dot{\gamma}_1 = 3.64 \times 10^{-6} SEC^{-1}$
$\dot{\gamma}_2 = 3.64 \times 10^{-4} SEC^{-1}$
ORDERED
$\dot{\gamma}_1 = 3.64 \times 10^{-6} SEC^{-1}$
$\dot{\gamma}_2 = 3.64 \times 10^{-4} SEC^{-1}$
$\tau^*/\tau_p^o \times G(0)/G(T)$
$U_n/2U_k \approx T/T_c$
0
0.1
0.2
0.3
0.4
0.5
0.6
0.7
0.8
0.9
1.0
0.2
0.4
0.6
0.8
1.0
1.2
1.4

FIG. 8

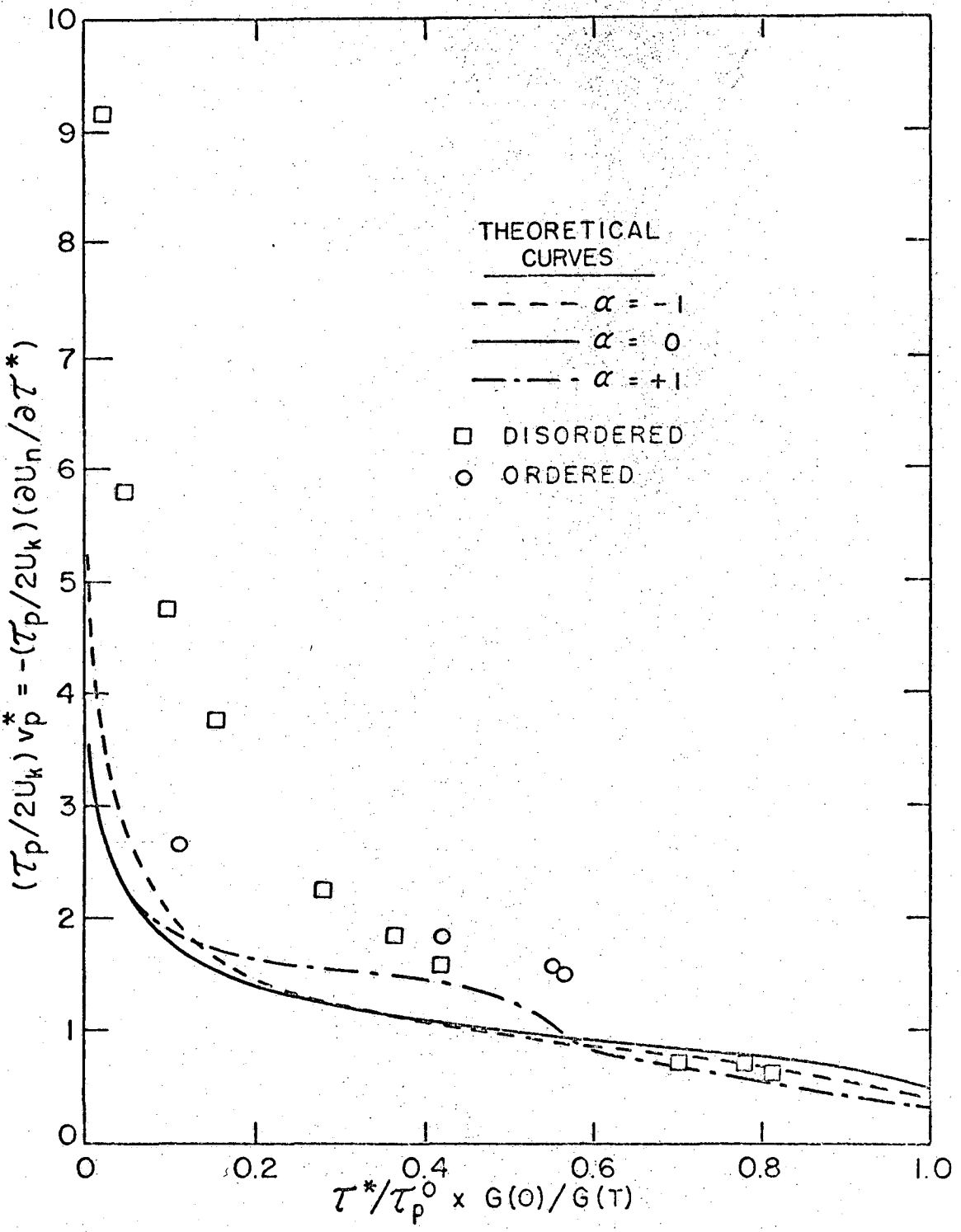
THEORETICAL CURVES
α = -1
α = 0
α = +1
DISORDERED
ORDERED
$(\tau_p/2U_k)\, v_p^* = -(\tau_p/2U_k)(\partial U_n/\partial \tau^*)$
$\tau^*/\tau_p^o \times G(0)/G(T)$
0
0.2
0.4
0.6
0.8
1.0
1
2
3
4
5
6
7
8
9
10

FIG. 9

This report was prepared as an account of Government sponsored work. Neither the United States, nor the Commission, nor any person acting on behalf of the Commission:

A. Makes any warranty or representation, expressed or implied, with respect to the accuracy, completeness, or usefulness of the information contained in this report, or that the use of any information, apparatus, method, or process disclosed in this report may not infringe privately owned rights; or

B. Assumes any liabilities with respect to the use of, or for damages resulting from the use of any information, apparatus, method, or process disclosed in this report.

As used in the above, "person acting on behalf of the Commission" includes any employee or contractor of the Commission, or employee of such contractor, to the extent that such employee or contractor of the Commission, or employee of such contractor prepares, disseminates, or provides access to, any information pursuant to his employment or contract with the Commission, or his employment with such contractor.